Isolation of *S. cerevisiae* snRNPs: Comparison of U1 and U4/U6.U5 to Their Human Counterparts

Patrizia Fabrizio, Sybille Esser, Berthold Kastner, Reinhard Lührmann

Small nuclear ribonucleoprotein (snRNP) particles are essential for pre–messenger RNA splicing. In human HeLa cells, 40 proteins associated with snRNPs have been identified. Yet, the function of many of these proteins remains unknown. Here, the immunoaffinity purification of the spliceosomal snRNPs U1, U2, U4/U6.U5, and several nucleolar snRNP species from the yeast *Saccharomyces cerevisiae* is presented. The U1 and U4/U6.U5 snRNPs were purified extensively and their protein composition and ultrastructure analyzed. The yeast U1 snRNP is larger and contains three times more specific proteins than its human counterpart. In contrast, the size, protein composition, and morphology of the yeast and the human U4/U6.U5 snRNPs are significantly similar. The preparative isolation of yeast snRNPs will allow the cloning as well as genetic and phylogenetic analysis of snRNP proteins which will accelerate our understanding of their function.

Four snRNPs, U1, U2, U4/U6, and U5, are essential components of the spliceosome, the complex that catalyzes the splicing of pre-mRNA. The snRNPs have at least three important functions: (i) recognition of splicing sites and branchpoint sequences, (ii) folding of pre-mRNA into a reactive structure and alignment of splice sites, and (iii) possibly direct contribution to catalysis [reviewed in (*1–3*)]. In addition to snRNPs, several non-snRNP splicing factors have been identified that in conjunction with snRNPs are essential for these processes (*1–3*). Studies in yeast and HeLa have demonstrated that the small nuclear ribonucleic acid (snRNA) moieties of the snRNPs form the core structure of the spliceosome by means of a network of RNA-RNA interactions between the snRNAs themselves and snRNAs and the pre-mRNA. These RNA-RNA contacts in the spliceosome are highly dynamic and are formed and broken during the functional cycle of the spliceosome (assembly, splicing, and disassembly) (*1–3*).

In comparison, much less is known about the function of the snRNP proteins. It is clear from yeast genetics, as well as from biochemical studies in the HeLa in vitro splicing system, that these proteins play an important role in splicing (*1–3*). One possible function of snRNP proteins may be the stabilization or disruption of the base-pairing interactions described above. The snRNPs from HeLa cells have been isolated and characterized thoroughly and contain about 40 proteins. Eight of these proteins are shared by all snRNPs (common proteins), whereas the others are particle-specific proteins (*4*).

A disadvantage of the HeLa system for functional studies of spliceosomal proteins is that genetic analysis is not feasible. In yeast, on the other hand, genetic screening studies have thus far identified only a few snRNP proteins, most of them essential for splicing (*2*). The only common snRNP protein that has been cloned in yeast, the homolog of the human D1, was isolated fortuitously as a neighbor of the *PRP38* gene (*5*).

A biochemical method that allowed the isolation of yeast snRNPs in preparative amounts, and therefore the cloning and subsequent genetic analysis of the snRNP proteins, would accelerate our understanding of the function and structure of snRNP particles. We used immunoaffinity chromatography with antibodies to the 5′ m_3G cap (anti-m_3G) of snRNPs to isolate snRNPs from yeast *S. cerevisiae* whole cell extracts (*6*). This procedure involves binding snRNP particles to immobilized anti-m_3G and then subsequent desorption, under native conditions, with an excess of m^7G nucleoside (anti-m_3G cross-reacts with the m^7G nucleoside), essentially as described for the purification of snRNPs from HeLa cells (*6*).

The RNA composition of the m^7G eluate from such an anti-m_3G affinity column loaded with snRNPs at 200 mM KCl is shown (Fig. 1A). Several RNA species with lengths between 100 and about 1700 nucleotides can be distinguished. These RNA molecules bind almost quantitatively to the column by their m_3G cap, whereas they are barely detectable in the column flow-through. Ribosomal RNAs, which do not possess an m_3G cap, are found in the flow-through and are rarely observed in the m^7G eluate (*7*). Northern (RNA) blot analysis of the m^7G eluate revealed the presence of U1, U2, U4, U5 long (L), U5 short (S), and U6 spliceosomal snRNAs and a large amount of U3 small nucleolar RNA (snoRNA) (Fig. 1B) (*8*, *9*). It is likely that all or most of the other bands present in the m^7G eluate represent m_3G-capped nucleolar snRNAs required for preribosomal processing. For example, the RNA species that runs between U3 and U5L may be snR10, whereas the ladder of RNAs that run between U5L and U5S may be snR3, 4, 5, 8, and 9 [reviewed in (*9*)].

We examined the *S. cerevisiae* proteins associated with the RNAs found in the m^7G eluate (*10*). The protein components of purified yeast snRNPs were analyzed by SDS–polyacrylamide gel electrophoresis (SDS-PAGE) and compared with those of purified snRNPs from HeLa cells. Roughly 50 to 60 individual proteins with molecular masses ranging from 10 kD to more than 200 kD could be clearly distinguished (Fig. 1C). Compared with HeLa spliceosomal snRNPs (Fig. 1C), the larger number of yeast proteins may be the result of the isolation of both spliceosomal and nucleolar snRNPs.

With an additional purification step (glycerol gradient fractionation) we obtained individual snRNPs in almost pure form. The RNA analysis of total snRNPs obtained from the 200 mM salt m^7G eluate of the immunoaffinity column, subsequently fractionated on a glycerol gradient at 200 mM KCl, is shown in Fig. 2A, upper panel. Under these conditions, the U1 snRNP was the fastest sedimenting snRNP particle and had a Svedberg value of about 18. The identity of the U1 RNA was confirmed by Northern blot analysis (*7*, *8*). Fraction 16 contained almost pure U1 snRNP (Fig. 2A).

Figure 2B (upper panel) shows an RNA analysis of snRNPs obtained from the 100 mM salt m^7G eluate of the immunoaffinity column that were subsequently fractionated on a glycerol gradient at 200 mM KCl. Under these conditions, far less U1 snRNP appeared in the eluate. The bulk of the U1 snRNP appeared to be lost in the flow-

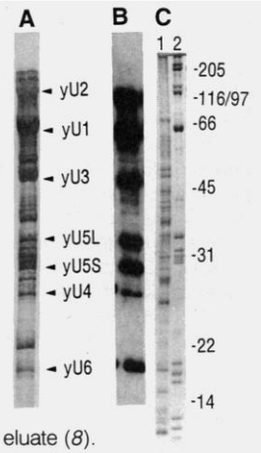

Fig. 1. Affinity purification of m_3G-capped snRNPs from whole cell extracts of yeast *S. cerevisiae*. (**A**) Silver staining of snRNAs eluted from the anti-m_3G affinity column was as described (*8*). The five spliceosomal yeast (y) RNAs U1 to U6 and the snoRNA U3 are labeled on the right. (**B**) Northern blot analysis of the same eluate (*8*). Exposure was for 40 min at −80°C. (**C**) Total spliceosomal proteins from HeLa (lane 2) and yeast (lane 1) m^7G eluate of the m_3G affinity column were stained with Coomassie blue. Molecular sizes are in kilodaltons.

Institut für Molekularbiologie und Tumorforschung, Philipps-Universität, D-35037 Marburg, Germany.

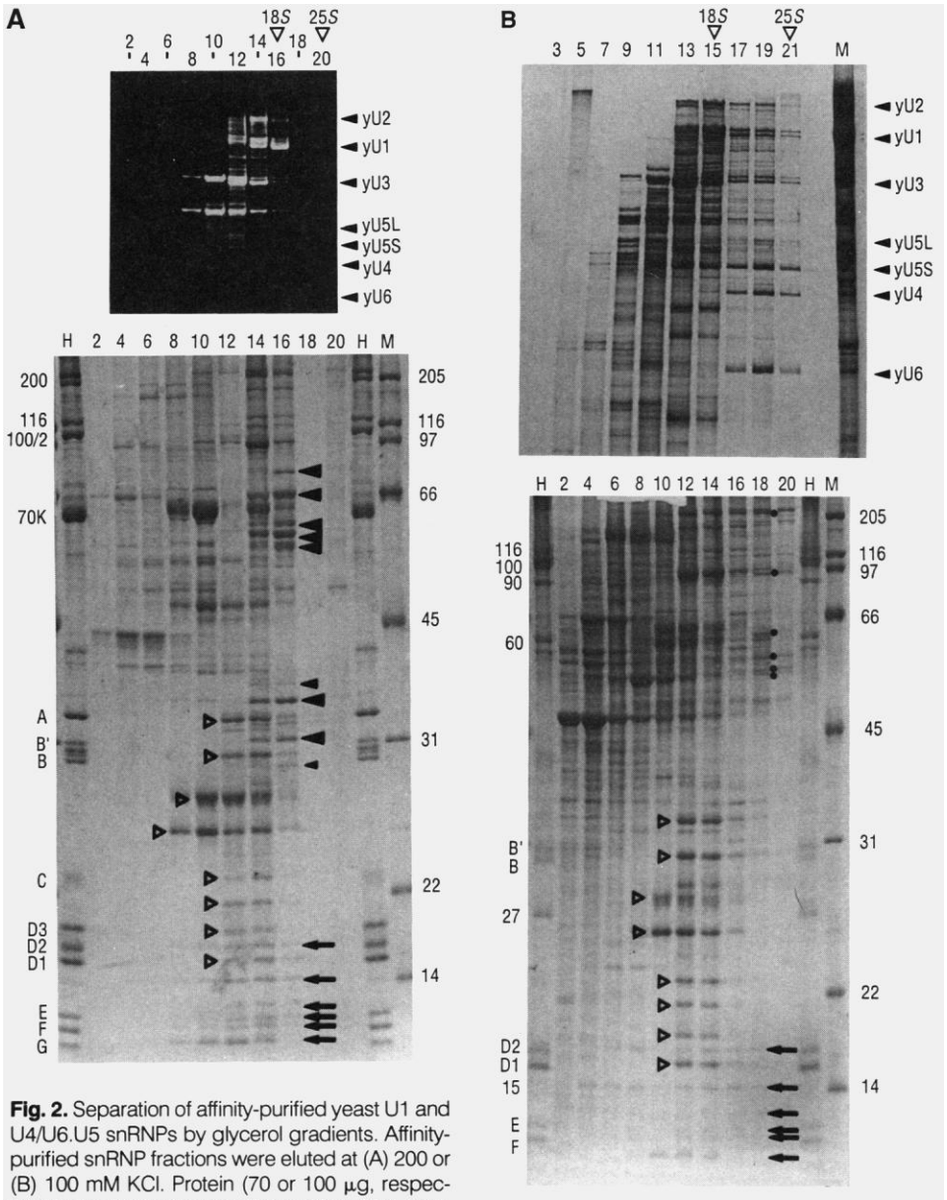

Fig. 2. Separation of affinity-purified yeast U1 and U4/U6.U5 snRNPs by glycerol gradients. Affinity-purified snRNP fractions were eluted at (A) 200 or (B) 100 mM KCl. Protein (70 or 100 μg, respectively) was layered onto a linear 10 to 30% glycerol gradient in buffer containing 20 mM Hepes-KOH (pH 7.9), 200 mM KCl, 1.5 mM $MgCl_2$, 0.5 mM DTT, pepstatin (4 μg/ml), and RNAsin (10 U/ml). The gradient was centrifuged in a Beckman SW40 rotor at 29 krpm for 24 hours. Fractions (500 μl) were collected from the top, and PCA extracted for analysis of RNA (upper panels) and proteins (lower panels) (*8, 10*). (**A**) (Upper panel) Ethidium bromide staining of RNAs. The five spliceosomal yeast (y) RNAs U1 to U6 and the snoRNA U3 are labeled on the right. The RNA species running just above U1 RNA may be snR30 snoRNA (*9*). The RNA species running just above U3 snoRNA may be a previously isolated RNA called 18b (*22*). The RNA species running between U3 and U5 long (L) may be snR10 snoRNA (*9*). (Lower panel) Coomassie blue staining of proteins. M, molecular size markers in kilodaltons and H, total HeLa spliceosomal snRNP proteins. The main HeLa proteins are labeled on the left. B, B′, D1, D2, D3, E, F, and G are the common core proteins. Arrows (→) indicate candidates for yeast U1 snRNP common core proteins; molecular sizes are 10, 11, 11.5, 12, 15, and 17 kD, respectively. Open arrowheads (▷) indicate candidates for snoRNP proteins. Large arrowheads (▶) indicate candidates for yeast U1 snRNP–specific proteins; molecular sizes are 32, 36, 54, 57, 60, 69, and 77 kD, respectively. The 34-kD protein running between the 32- and the 36-kD proteins is a candidate for the yeast 70K protein SNP1 (*17*). Small arrowheads (▶) indicate candidates for additional yeast U1-specific proteins; molecular sizes are 27.5 and 38 kD. The 38-kD protein is a candidate for the yeast A protein (*18*). (**B**) (Upper panel) Silver staining of RNAs. The five spliceosomal yeast (y) RNAs U1 to U6 and the snoRNA U3 are labeled on the right. M, marker consisting of the RNAs from total snRNPs before fractionation in the gradient. (Lower panel) Coomassie blue staining of proteins. M, molecular size markers. H, total HeLa U4/U6.U5 tri-snRNP proteins. The main HeLa U4/U6.U5 proteins are labeled on the left. Arrows (→) indicate candidates for yeast U4/U6.U5 common core proteins; molecular sizes are 10, 11, 11.5, 12, 15, and 17 kD, respectively. Open arrowheads (▷) indicate candidates for snoRNP proteins. Dots (●) indicate candidates for yeast U4/U6.U5 snRNP–specific proteins; molecular sizes are 51, 52, 56, 62, 97, and 280 kD, respectively.

through during column loading at 100 mM salt, probably because the U1 snRNP interacts with other spliceosomal components under these conditions, which makes the m_3G cap of U1 unavailable for anti-m_3G. We obtained a 25S fraction substantially enriched in U4/U6.U5 tri-snRNP complex (fraction 19), as determined by RNA gel analysis (Fig. 2B), using 100 mM salt during affinity chromatography. Again, the identity of RNAs was verified by Northern blot analysis (*7*). It was interesting that the U4/U6.U5 tri-snRNP could be isolated in the absence of adenosine triphosphate (ATP), because earlier studies had shown that the depletion of ATP from yeast extracts inhibited the formation of the U4/U6.U5 complex (*11*). Other studies have shown that U4/U6 and U5 snRNPs associate in the splicing extract and that U5 dissociates from the U4/U6 snRNPs on addition of ATP (*12*).

The protein composition of fractions from the two glycerol gradients is shown in Fig. 2, A and B (lower panels). We have detected at least six candidates for common proteins, which by definition must be present both in the U1 snRNP and the U4/U6.U5 tri-snRNPs. Depending on the isolation conditions, we often detected double bands for some of the common proteins, suggesting that the number of these proteins may be higher. The yeast common proteins are barely visible after staining with Coomassie blue, but they are seen clearly in silver-stained gels (*7*).

The similarity between the molecular masses of yeast and HeLa common proteins, in particular in the 20- and 10-kD regions, makes it likely that the yeast homologs of the HeLa E, F, and G proteins have similar sizes. Our observations that affinity-purified antiserum to human F protein (anti-F) strongly cross-reacts with a yeast protein of similar molecular mass as the human F protein are consistent with this proposal (*7*). Additional proteins of low molecular mass that do not cosediment with the U1 and the U4/U6.U5 snRNPs but that do with the U3 and the other snoRNPs can be seen interspersed between these putative yeast common proteins (Fig. 2, A and B). Therefore, it is likely that they are of nucleolar origin.

The lower panel of Fig. 2A also shows the candidates for U1-specific proteins. We observed about seven proteins that clearly cosediment with the yeast U1 snRNA (Fig. 2A, lower panel, fraction 16). These seven U1-specific proteins have molecular masses ranging from 32 to 77 kD. Moreover, at least two additional proteins cosediment with the U1 snRNA in fraction 16. These proteins, although less abundant, may also be U1-specific proteins (Fig. 2A).

In contrast, the U4/U6.U5 complex re-

vealed a protein pattern that was similar to, or possibly less complex than, that of the human tri-snRNP (Fig. 2B, lower panel). When compared with the U1 snRNP, the amount of the U4/U6.U5 snRNP obtained is low and the preparation relatively less pure. Therefore, the exact number of proteins cannot be determined. With further improvements in the purification and enrichment scheme, it should be possible to isolate additional proteins. The U4/U6.U5 tri-snRNP RNAs peak in fraction 19 (Fig. 2B, upper panel). About six proteins cosediment with these RNAs (Fig. 2B, lower panel). These proteins have molecular masses ranging from 51 to 280 kD. Some of these proteins may be the yeast PRP tri-snRNP proteins isolated earlier (*2*). On the basis of Western blot analysis [below and (*7*)], there is evidence suggesting that the 280-kD protein is PRP8, the 97-kD protein PRP6, and the 52-kD protein PRP4 (*11, 13, 14*).

We tested whether proteins associated with the yeast U4/U6.U5 tri-snRNP or with the U3 snoRNP cofractionated with the isolated snRNPs in the gradient. Probing Western blots of glycerol gradient fractions with antibodies to PRP4 (anti-PRP4) and PRP6 (anti-PRP6) and antisera to human fibrillarin (anti-fibrillarin) (Fig. 3) confirmed the presence of all of these marker proteins at the expected position in the gradient. Proteins PRP4 and PRP6 sedimented in the 25S position together with the U4/U6.U5 tri-snRNP. Some PRP4 and PRP6 protein also sedimented at the top of the gradient, presumably as a result of the presence of uncomplexed protein or of protein associated solely with the U4/U6 snRNP. The yeast fibrillarin NOP1 protein is known to be part of the U3 and many other snoRNPs (*9, 15*). The anti-fibrillarin showed that the yeast equivalent is indeed sedimenting together with the U3 snoRNP at a sedimentation value of 10 to 12S. Thus, PRP4 and PRP6 cosediment with the U4/U6.U5 tri-snRNP, and NOP1 with the U3 snoRNP or with the other snoRNPs after gradient sedimentation.

In summary, like their human counterparts, the yeast U1 and U4/U6.U5 snRNPs appear to be composed of two classes of proteins: common and specific proteins. At this stage of purification, the yeast U4/U6.U5 snRNP has a protein composition probably of similar complexity as the human tri-snRNP. In contrast, the yeast U1 snRNP seems to have a more complex biochemical composition than its human counterpart, with seven to nine candidate specific proteins.

The purity of U1 and the substantial enrichment of the U4/U6.U5 tri-snRNP preparations allowed us to investigate their structures by electron microscopy and to compare their morphology with that of their human homologs. We investigated in detail not only the complexity of the yeast U1 snRNP but also the structure and shape of the yeast U4/U6.U5 tri-snRNP.

Typical images of negatively stained yeast U4/U6.U5 snRNPs are shown (Fig. 4A). They show an elongated body, up to 30 nm long, with one pointed end and a broader, head-like structure. In addition, there is a protuberance pointing to the upper left in most of the images. The images in the last row show additional globular structures instead of the protuberance. The general appearance of the yeast U4/U6.U5 snRNP is very similar to the HeLa counterpart which is shown for comparison. Similar structural details are recognizable: the main body with pointed and broad ends and the protuberance or the globular structures. However, the cleft between body and protuberance in the HeLa species in most images is less pronounced than in the yeast U4/U6.U5 snRNP. Often the cleft is not visible at all. The body of the HeLa U4/U6.U5 snRNP is also slightly shorter, giving the particle a length of up to 25 nm.

In contrast to the U4/U6.U5 snRNP, the U1 snRNP differs pronouncedly in

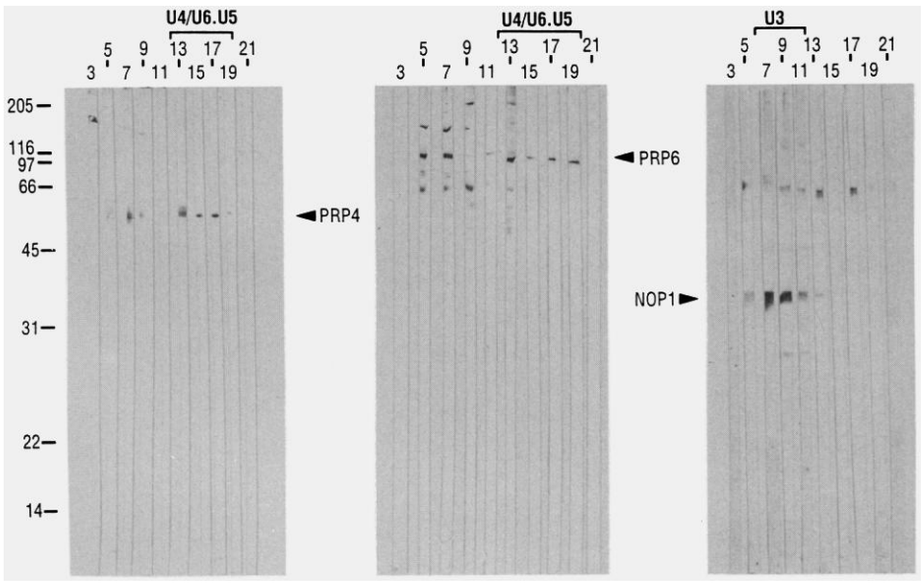

Fig. 3. PRP4 and PRP6 cosediment with the yeast U4/U6.U5 snRNP on glycerol gradients, and the yeast fibrillarin homolog (NOP1) cosediments with the yeast U3 snoRNP. The snRNPs were eluted from the m_3G affinity column at 100 mM KCl. Gradients were performed at 200 mM KCl as described in the legend to Fig. 2 except that the run was for 18 hours at 29 krpm. Proteins from the gradient fractions were blotted on nitrocellulose as described (*21*). Each lane was cut in three strips, and each strip was probed with anti-PRP4, anti-PRP6, or anti-fibrillarin, respectively. PRP4 has a molecular mass of 52 kD, PRP6 of 104 kD, and NOP1 of 38 kD (*13–15*). The silver-stained RNA gel from the same gradient fractions showed that the U3 and other snoRNAs sediment in fractions 7 to 9, and the U4, U6, and U5 snRNAs peak in fractions 15 to 17 (*7*). Molecular sizes are indicated to the left in kilodaltons.

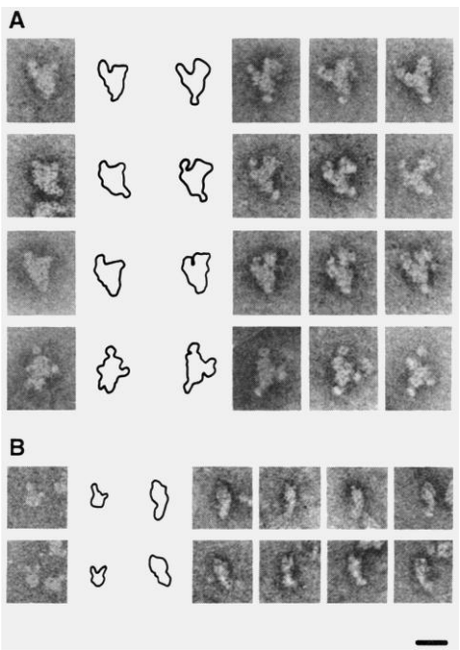

Fig. 4. Images of negatively stained U1 and U4/U6.U5 snRNPs. Typical images of yeast U1 and U4/U6.U5 snRNPs are shown on the right panel. For comparison, images of their human counterparts are shown on the left panel. (**A**) U4/U6.U5 snRNP. (**B**) U1 snRNP. Scale bar, 20 nm. Negative staining with 2.5% uranyl formate was carried out by the double-carbon film method as described (*16*). The preparations were examined under a Zeiss EM 109 electron microscope with an acceleration voltage of 80 kV. Electron micrographs were taken at ×85,000 and ×140,000.

structure and size between the two species. Yeast U1 snRNP has an elongated structure of about 20 nm in length and 8 to 10 nm wide (Fig. 4B). The structure can be divided into a more globular domain and a bent, elongated domain. In most images this domain leaves the body with a bend to the right side, more rarely to the left. HeLa U1 snRNP in comparison is much smaller, consisting of a main body of about 8 nm in diameter with two small protuberances (*16*). By specific depletion and labeling experiments it has been shown that the U1-specific proteins 70K and A, respectively, are contained in the two protuberances (*16*). Yeast proteins potentially homologous to these have recently been identified, so that these proteins may also be present in the yeast U1 snRNP (Fig. 2A) (*17, 18*). It is not clear whether these proteins create protuberances similar to those seen in the HeLa U1 snRNPs, as fine structures similar to the HeLa protuberances could be recognized in only a few of the yeast U1 snRNP images.

The composition of the yeast U1 snRNP is complex when compared with the human U1 snRNP, which contains only three specific proteins (*4*). Both the biochemical compositions and the shapes of the yeast and the human U1 snRNP show significant differences, which could reflect functional differences. In both systems, the U1 snRNP is important for early assembly events. In yeast, the selection of splice sites is rather simple compared with the human system. There are no examples of alternatively spliced mRNAs in yeast, in which most of the interrupted genes contain a single, constitutively spliced intron. As a consequence, the very early steps of splice-site recognition in yeast could be organized in a more rigid manner because discrimination between several candidate sites is not necessary. The yeast 18S U1 snRNP that we have isolated could thus represent a preassembled complex required for commitment of pre-mRNA to splicing (*19*). By contrast, in mammals a multitude of patterns of alternative splicing have been reported (*20*). The U1 snRNP has to adapt to each of these patterns by assembling into a specific commitment complex each time. Therefore, in the mammalian system the initial steps of splice-site recognition must be regulated with more versatility than in yeast.

In contrast, the yeast U4/U6.U5 snRNP shows a structural similarity to its human counterpart. Electron microscopy showed that the general architecture as well as structural details appear to be conserved between the yeast and the human U4/U6.U5 snRNPs. This large amount of structural similarity is consistent with the evolutionary conservation of the splicing mechanism between species. In yeast, as in mammals, the tri-snRNP U4/U6.U5 enters the spliceosome late, after the binding of U1 and U2 snRNPs to pre-mRNA (*1, 2*). The U6 snRNA is critical during the splicing process and believed to be part of the catalytic center of the spliceosome (*2*). Therefore, it is possible that the structure of the human and the yeast U4/U6.U5 snRNPs is conserved because the steps of spliceosome assembly in which they participate are also highly conserved, requiring not only sequence but also structural conservation. This hypothesis would be strengthened if it could be shown that the splicing activity of a U4/U6.U5-depleted HeLa extract is restored by the addition of purified yeast tri-snRNP and vice versa.

Pure U2 snRNPs could not be obtained at this stage because this particle comigrates with other snRNPs, in particular with the nucleolar snRNPs (Fig. 2A). Additional purification steps, such as oligonucleotide affinity chromatography, will be required to purify U2 and the nucleolar snRNPs further.

The isolation of yeast snRNPs under native conditions presented here promises to be an important step in the characterization of the yeast snRNP proteins by straightforward biochemical methods. Because large amounts of snRNP proteins can now be isolated, microsequencing should allow their genes to be cloned. The high evolutionary conservation of the splicing mechanism between yeast and human will then allow the exploitation of both yeast genetics and biochemistry. Exchanging components or protein domains will accelerate the identification of homologous, functionally important domains of some snRNP proteins; thus, yeast may be used as a biological trap to capture conserved components of the human splicing apparatus.

REFERENCES AND NOTES

1. M. R. Green, *Annu. Rev. Cell Biol.* **7**, 559 (1991); M. J. Moore, C. C. Query, P. A. Sharp, in *The RNA World*, R. F. Gesteland and J. F. Atkins, Eds. (Cold Spring Harbor Press, Cold Spring Harbor, NY, 1993), pp. 303–357.
2. C. Guthrie, *Science* **253**, 157 (1991); S. W. Ruby and J. Abelson, *Trends Genet.* **7**, 79 (1991); B. C. Rymond and M. Rosbash, in *The Molecular and Cellular Biology of the Yeast* Saccharomyces, E. W. Jones, J. R. Pringle, J. R. Broach, Eds. (Cold Spring Harbor Press, Cold Spring Harbor, NY, 1992), pp. 143–192.
3. R. Lührmann, B. Kastner, M. Bach, *Biochim. Biophys. Acta* **1087**, 265 (1990).
4. The HeLa U1 snRNP has consistently been isolated as a 12*S* particle containing three U1-specific proteins named 70K, A, and C [M. Hinterberger, J. Pettersson, J. A. Steitz, *J. Biol. Chem.* **258**, 2604 (1983); P. Bringmann and R. Lührmann, *EMBO J.* **5**, 3509 (1986)]. Two distinct forms of the U2 snRNP particle have been isolated: a 12*S* form containing two U2-specific proteins named A′ and B″ and a 17*S* form that contains nine additional U2-specific proteins with molecular masses ranging from 35 to 160 kD [S.-E. Behrens, K. Tyc, B. Kastner, J. Reichelt, R. Lührmann, *Mol. Cell. Biol.* **13**, 307 (1993)]. The U4/U6 and U5 snRNPs have been isolated as individual 12*S* or 20*S* particles, respectively. At low ionic strength, a 25*S* tri-snRNP complex that contains seven proteins with molecular masses ranging from 15.5 to 90 kD, not present in 20*S* U5 or 12*S* U4/U6 snRNPs, is observed [M. Bach, G. Winkelmann, R. Lührmann, *Proc. Natl. Acad. Sci. U.S.A.* **86**, 6038 (1989); S.-E. Behrens and R. Lührmann, *Genes Dev.* **5**, 1439 (1991)].
5. B. C. Rymond, *Proc. Natl. Acad. Sci. U.S.A.* **90**, 848 (1993).
6. The yeast strain EJ101 (*α his1 prb-1122 prc1-126*) was propagated at 30°C in YPD medium at a density of A_{600} = 3 to 5 (absorbance, *A*, measured at 600 nm). Extracts were prepared as described [R.-J. Lin, A. J. Newman, S.-C. Cheng, J. Abelson, *J. Biol. Chem.* **260**, 14780 (1985)]. Routinely, 16 liters of culture were grown (~160 g of cells) that yielded 100 ml of splicing extract. Affinity purification of m_3G-capped snRNPs from whole cell extracts was performed with anti-m_3G (monoclonal antibody H20) bound covalently to CNBr-activated Sepharose 4B essentially as described [M. Bach, P. Bringmann, R. Lührmann, *Methods Enzymol.* **181**, 232 (1990)]. Whole cell extract prepared as above was diluted to reduce the concentration of glycerol to 8% and passed over a H20 Sepharose column in a buffer containing 20 mM Hepes-KOH (pH 7.9)], 0.2 mM EDTA (pH 8.0), 0.5 mM dithiothreitol (DTT), pepstatin (4 μg/ml), 8% glycerol, and 50, 100, or 200 mM KCl depending on the conditions required. Bound snRNPs were eluted with 20 mM m^7G nucleoside and KCl concentrations ranging from 100 to 400 mM, as required. The yield was 150 to 270 μg of protein on elution of bound snRNPs.
7. P. Fabrizio, S. Esser, R. Lührmann, unpublished data.
8. Samples were extracted with 1 volume of PCA (phenol, chloroform, isoamylalcohol 50:50:1). For Northern blots, RNA was fractionated by electrophoresis on 8% polyacrylamide gels containing 8 M urea and transferred to nylon membrane (Qiabrane) by electrophoresis in 25 mM sodium phosphate (pH 6.5) for 18 to 20 hours at 22 V and fixed by ultraviolet irradiation. Probes to the yeast U1, U2, U3, U4, U5, and U6 snRNAs were made by the random priming method with a kit from Stratagene. Prehybridization and hybridization procedures were performed as described [P. Fabrizio, D. S. McPheeters, J. Abelson, *Genes Dev.* **3**, 2137 (1989)]. Alternatively, we visualized RNA by staining with silver [C. R. Merril, *Methods Enzymol.* **182**, 477 (1990)] or ethidium bromide.
9. M. J. Fournier and E. S. Maxwell, *Trends Biochem. Sci.* **18**, 131 (1993).
10. Proteins were precipitated from the organic phase of the PCA extraction with 5 volumes of acetone and were fractionated by 12% SDS-PAGE. To resolve small proteins, we polymerized gels in the presence of high TEMED concentrations (*21*). Protein bands were detected with Coomassie brilliant blue G250 stain or silver stain [W. Wray, T. Boulikas, V. P. Wray, R. Hancock, *Anal. Biochem.* **118**, 197 (1981)].
11. M. Lossky, G. J. Anderson, S. P. Jackson, J. Beggs, *Cell* **51**, 1019 (1987).
12. S.-C. Cheng and J. Abelson, *Genes Dev.* **1**, 1014 (1987).
13. P. Legrain and A. Choulika, *EMBO J.* **9**, 2775 (1990); N. Abovich, P. Legrain, M. Rosbash, *Mol. Cell. Biol.* **10**, 6417 (1990).
14. J. Banroques and J. N. Abelson, *Mol. Cell. Biol.* **9**, 3710 (1989); S. P. Bjorn, A. Soltyk, J. D. Beggs, J. D. Friesen, *ibid.*, p. 3698.
15. R. P. Jansen *et al.*, *J. Cell Biol.* **113**, 715 (1991).
16. B. Kastner and R. Lührmann, *EMBO J.* **8**, 277 (1989); B. Kastner, U. Kornstädt, M. Bach, R. Lührmann, *J. Cell Biol.* **116**, 839 (1992).
17. V. Smith and B. G. Barrell, *EMBO J.* **10**, 2627 (1991).
18. X. C. Liao, J. Tang, M. Rosbash, *Genes Dev.* **7**, 419 (1993).
19. B. Séraphin and M. Rosbash, *Cell* **59**, 349 (1989).
20. T. Maniatis, *Science* **251**, 33 (1991).
21. T. Lehmeier, K. Foulaki, R. Lührmann, *Nucleic Acids Res.* **18**, 6475 (1990).
22. N. Riedel, J. A. Wise, H. Swerdlow, A. Mak, C.

Guthrie, *Proc. Natl. Acad. Sci. U.S.A.* **83**, 8097 (1986).
23. We thank H. Hermann for anti-F, J. Banroques and P. Legrain for anti-PRP4 and anti-PRP6, and G. Reimer for anti-fibrillarin. We thank B. Lübben for help with the m_3G immunoaffinity column and I. Öchsner-Welpelo for technical assistance. We also thank W. Hackl, M. Jahn, C. Marshallsay, C. Will, and P. Wooley for critical reading of this manuscript. Supported by grants from the Deutsche Forschungsgemeinschaft (SFB 272/73), the Alexander-von-Humboldt-Stiftung, and the Fonds der Chemischen Industrie.

27 December 1993; accepted 28 February 1994

Mutational Isolation of a Sieve for Editing in a Transfer RNA Synthetase

Eric Schmidt and Paul Schimmel

Editing reactions are essential for the high fidelity of information transfer in processes such as replication, RNA splicing, and protein synthesis. The accuracy of interpretation of the genetic code is enhanced by the editing reactions of aminoacyl transfer RNA (tRNA) synthetases, whereby amino acids are prevented from being attached to the wrong tRNAs. Amino acid discrimination is achieved through sieves that may overlap with or coincide with the amino acid binding site. With the class I *Escherichia coli* isoleucine tRNA synthetase, which activates isoleucine and occasionally misactivates valine, as an example, a rationally chosen mutant enzyme was constructed that lacks entirely its normally strong ability to distinguish valine from isoleucine by the initial amino acid recognition sieve. The misactivated valine, however, is still eliminated by hydrolytic editing reactions. These data suggest that there is a distinct sieve for editing that is functionally independent of the amino acid binding site.

Editing reactions in information transfer have long been recognized (*1–5*), and those associated with tRNA synthetases were among the first to be investigated (*3*, 6–8). The aminoacylation reaction occurs in two steps: (i) an amino acid activation reaction in which an amino acid is condensed with adenosine triphosphate (ATP) to form an aminoacyl adenylate and (ii) the transfer reaction in which the aminoacyl moiety is transferred from the adenylate to the tRNA substrate cognate to the amino acid (*9*). The overall accuracy of aminoacylation depends on the specificity of amino acid activation (first sieve) and on pre- and posttransfer editing events (second sieve), which correct for occasional errors of amino acid activation (*3*, 6, *10*). *Escherichia coli* isoleucine tRNA synthetase (IleRS) is a 939–amino acid monomeric class I tRNA synthetase (*11*) that misactivates the closely related valine at a relative frequency of about 0.5% (*12*). When presented with $tRNA^{Ile}$, the enzyme-bound misactivated valyl–adenosine monophosphate (Val-AMP) is hydrolyzed either directly or by transient formation of Val-$tRNA^{Ile}$ followed by rapid deacylation of the mischarged species (*13–17*). These pre- and posttransfer editing events are manifested by a $tRNA^{Ile}$-dependent hydrolysis of ATP in the presence of valine (*17*).

In spite of considerable progress on the elucidation of structures of class I and class II tRNA synthetases (*18–23*), the structural basis for editing has not been revealed. One difficulty has been the lack of crystal structures for free amino acid or aminoacyl-tRNA complexed with the cognate enzyme. Because both the first sieve and the pre- and posttransfer editing of the second sieve show strong amino acid discrimination, the structural basis for both sieves, although unknown, has been assumed to be connected in some way with an amino acid binding site (*15*).

Although not determined, the three-dimensional structure of IleRS is believed to be most related to that of methionine tRNA synthetase (*11*). On the basis of the close evolutionary relation between these enzymes, a model for the active site region of IleRS has been developed (*24–27*). The nucleotide binding fold of alternating β strands and α helices that characterizes the class I tRNA synthetases incorporates one (the 11–amino acid signature sequence) of the two class-defining sequence motifs into a loop between the first strand (β_A) and helix (α_A), and this segment in turn forms part of the ATP interaction site (*21*). Mutational analysis of *E. coli* methionine tRNA synthetase shows that this region also contributes to amino acid binding (*25*). We confirmed the significance of this part of the structure for interaction with the aminoacyl moiety by determining that it can be cross-linked to the isoleucyl group of bound *N*-bromoacetyl isoleucyl-$tRNA^{Ile}$ (*28*). Within the 20 amino acids that form β_A and the following loop, position 56 is the only one at which IleRS and ValRS have a different and yet strictly conserved amino acid (Gly^{56} and Pro, respectively) (*26*). With this in mind, we introduced substitutions at position 56 to see whether these substitutions affected isoleucine versus valine discrimination and the editing reactions.

A Gly^{56} to Ala substitution (G56A) (*29*) completely eliminated the discrimination between isoleucine and valine in the

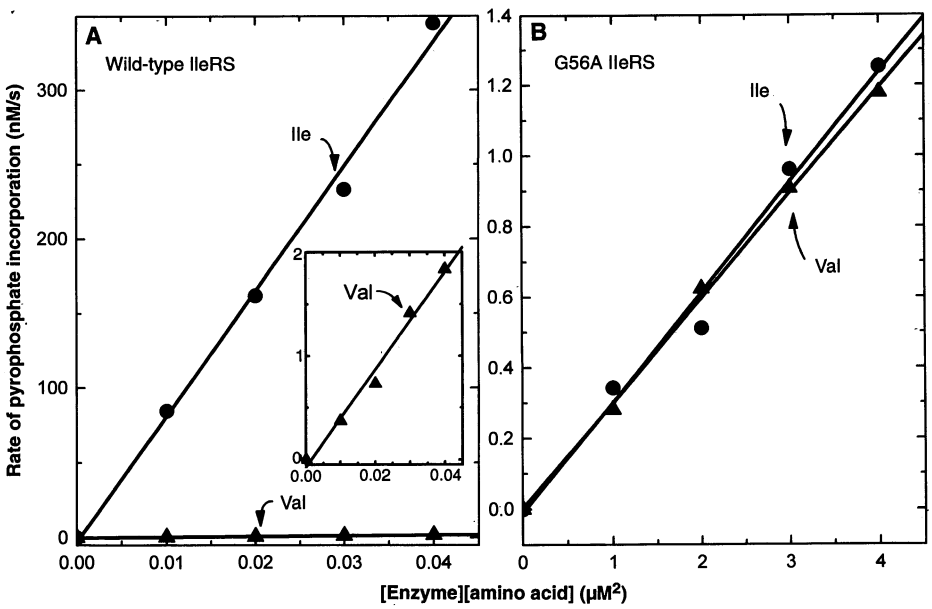

Fig. 1. Amino acid activation activities for wild-type (**A**) and G56A (**B**) IleRS. The inset of (A) gives an expanded scale to show detection of amino acid activation with valine. Initial rates of pyrophosphate incorporation into ATP are plotted versus the product of the enzyme and amino acid concentrations. The slope of the graph is equal to the second-order rate constant k_{cat}/K_m.

Department of Biology, Massachusetts Institute of Technology, Cambridge, MA 02139, USA.